Loss of function of an Arabidopsis homolog of *JMJD6*, suppresses the dwarf phenotype of *acl5*, a mutant defective in thermospermine biosynthesis.

Hirotoshi Matsuo, Hiroko Fukushima, Shinpei Kurokawa, Eri Kawano, Takashi Okamoto, Hiroyasu Motose and Taku Takahashi

Graduate School of Natural Science and Technology, Okayama University, Okayama 700 8530, Japan

Correspondence
T. Takahashi, Graduate School of Natural Science and Technology, Okayama University, Okayama 700 8530, Japan
Tel: +81 86 251 7858
E-mail: perfect@cc.okayama-u.ac.jp

Abstract

In *Arabidopsis thaliana*, the *ACL5* gene encodes thermospermine synthase and its mutant, *acl5*, exhibits a dwarf phenotype with excessive xylem formation. Studies of suppressor mutants of *acl5* reveal the involvement of thermospermine in enhancing mRNA translation of the *SAC51* gene family. We show here that a mutant, *sac59*, which partially suppresses the *acl5* phenotype, has a point mutation in *JMJ22* encoding a D6-class Jumonji C protein. A T-DNA insertion allele, *jmj22-2*, also partially suppressed the *acl5* phenotype while mutants of its closest two homologs *JMJ21* and *JMJ20* had no such effects, suggesting a unique role of JMJ22 in plant development. We found that mRNAs of the *SAC51* family are more stabilized in *acl5 jmj22-2* than in *acl5*.

Keywords: Arabidopsis; JMJD6; mRNA stability; thermospermine; xylem development

Abbreviations

ACL5, ACAULIS5; CaMV, cauliflower mosaic virus; Col-0, Columbia-0; JMJ, JUMONJI; GO, Gene Ontology; L*er*, Landsberg *erecta*; NMD, nonsense-mediated mRNA decay; SAC, suppressor of *acl5*; SPMS, spermine synthase; uORF, upstream open reading frame

Introduction

Thermospermine, a structural isomer of spermine, was first discovered in an extreme thermophile, *Thermus thermophilus* [1], and is known to be present ubiquitously in the plant kingdom [2]. The mutant of the *ACAULIS5* (*ACL5*) gene, which encodes thermospermine synthase in *Arabidopsis thaliana*, exhibits severe dwarfism with increased vein thickness and vascularization in all organs and exogenous treatment with thermospermine partially restores the mutant phenotype [3]. A study of the *thickvein* (*tkv*) mutant, an allele of *ACL5*, suggests that the boundary between veins and nonvein regions is defined by *ACL5/TKV* whose expression is specific to provascular cells [4]. Isolation and characterization of suppressor mutants named *suppressor-of-acl5* (*sac*), which restore the dwarf phenotype of *acl5*, have revealed that thermospermine is involved in the upstream open reading frame (uORF)-mediated translational control of the *SAC51* gene which encodes a basic helix-loop-helix (bHLH) protein and contains multiple uORFs within the 5' leader region of the mRNA [5]. One of these uORFs is highly conserved among all four members of the *SAC51* gene family in Arabidopsis and those in different plant species. This uORF has an inhibitory effect on the main ORF translation, while thermospermine plays a role in counteracting this effect. The *sac51-d* dominant allele, which completely suppresses the *acl5* phenotype, contains a premature termination codon in the conserved uORF. Studies of *sac52-d*, *sac53-d*, and *sac56-d* dominant mutants whose responsible genes encode ribosomal proteins, RPL10A, RACK1A, and RPL4A, respectively, have shown that these mutations attenuate the inhibitory effect of the *SAC51* uORF without thermospermine and result in stabilization of the *SAC51* mRNA [6, 7]. Furthermore, point mutations in the conserved uORFs of two members of the *SAC51* family, *SACL1* and *SACL3*, were also identified as dominant suppressors of *acl5* [8, 9]

On the other hand, heterodimers of bHLH transcription factors of LONESOME HIGHWAY (LHW) and auxin-induced TARGET OF MONOPTELOS5 (TMO5) or TMO5-LIKE1 (T5L1) are known to direct xylem differentiation in Arabidopsis [10]. These dimers also regulate expressions of *ACL5* and *SACL3*. The bHLH protein encoded by *SACL3* has been found to competitively interfere with TMO5/T5L1 binding to LHW and may be thus integrated with thermospermine into a negative feedback control of auxin-induced xylem formation [8,11]. However, the precise mode of action of thermospermine remains to be clarified.

To get further insight into the factors associated with thermospermine-mediated repression of xylem differentiation, we have extended the analysis to additional mutants that suppress the *acl5* mutant phenotype. We report here on characterization of the *sac59* mutant, which is shown to represent a recessive allele of *JMJ22*. JMJ22 is a Jumonji C (JmjC) domain-containing protein belonging to the JMJD6 family, which plays an important developmental role in animals [12-16]. Although JMJD6 was first characterized as a phosphatidylserine

receptor responsible for engulfment of apoptotic cells and then assigned a role as a histone arginine demethylase, there is accumulating evidence that JMJD6 binds to and modifies single-stand RNA [12, 17, 18]. While a study has shown that JMJD6 is involved in mRNA splicing as a lysine hydroxylase of U2AF65, a mediator of RNA splicing, another report has revealed that it has dual histone and snRNA demethylase activity on anti-pause enhancers regulating the RNA polymerase II function [19]. The Arabidopsis genome contains 21 genes encoding JmjC proteins [20, 21]. Among them, five JmjC proteins have been so far identified as histone H3 lysine 27 (H3K27) demethylases: JMJ11/EARLY FLOWERING 6 (ELF6), JMJ12/RELATIVE OF ELF6 (REF6), JMJ13, JMJ30, and JMJ32 but no JmjC proteins have been implicated in mRNA processing or metabolism. Our results provide evidence showing the involvement of plant JMJD6 in mRNA stability.

Materials and methods

Plant materials and growth conditions

Arabidopsis (*Arabidopsis thaliana*) accessions, Columbia-0 (Col-0) and Landsberg *erecta* (L*er*), were used as wild type. The *acl5* mutant allele, *acl5-1*, was originally isolated in the L*er* background and that in Col-0 was obtained by repeating the cross with the wild-type Col-0 more than seven times [22]. *sac59*, which we later renamed *jmj22-3*, was identified from an ethyl methanesulfonate (EMS)-mutagenized population of *acl5-1* as one of its suppressor mutants [7]. A T-DNA insertion allele of *JMJ20* (Salk_202511C) named *jmj20-2* and that of *JMJ22* (SAIL_448_F12) named *jmj22-2* were obtained from the Arabidopsis Biological Resource Center (ABRC, Columbus, OH, USA). Plants were grown on rock-wool cubes surrounded with vermiculite at 22°C under 16 h light/8 h dark conditions, unless otherwise indicated. For RNA preparation, seeds were surface-sterilized with bleach solution containing 0.01% Triton X-100 for 3 min, rinsed three times in sterile water, germinated on 0.8% agar plates supplemented with Murashige-Skoog (MS) nutrients (Wako, Tokyo, Japan) and 1% sucrose, and grown at 22°C under 16 h light/8 h dark conditions.

Identification of point mutation

Chromosome mapping of *sac59* was carried out as described [7]. Polymorphic markers used are described previously [23-25]. The mutation site was identified by whole sequencing of the

sac59 genomic DNA performed using the MGI DNBSEQ-G400 system at Bioengineering Lab. (Sagamihara, Japan).

Genome editing

A CRISPR/CAS9 construct for *JMJ21* knockout was made as described previously [26]. A pair of oligonucleotides CAS9JMJ21-F and CAS9JMJ21-R (Table S1) were annealed and ligated into the *Bbs*I restriction site of pEn-Chimera (Addgene, Cambridge, MA, USA). The resulting chimeric sequence was then transferred into pDe-CAS9 plant transformation vector (Addgene) by a single site Gateway LR reaction (Invitrogen, Carlsbad, CA, USA). The construct was introduced into wild-type Col-0 plants via *Agrobacterium*-mediated transformation [27]. Transgenic lines were selected for phosphinothricin resistance with 5 mg/L phosphinothricin (Sigma-Aldrich, St. Louis, MO, USA). CAS9-induced mutations were identified by PCR amplification of the *JMJ21* target region with a pair of primers, JMJ21-exF and JMJ21-exR (Table S1), followed by digestion of the DNA with *Bgl*II, which was designed in advance to locate several bp upstream of the PAM site, and detection of the polymorphism on agarose gels.

Genotyping

The genotype of each mutant was confirmed by PCR using gene-specific primers (Table S1) followed by agarose gel electrophoresis. *jmj22-3* and *acl5-1* alleles were detected by digesting the PCR fragments of the corresponding genes with *Bam*HI and *Xho*I, respectively, and resolving them on 4% agarose gels. Genotyping of *sac51-1* and *sacl3-1* was as described previously [9].

RNA extraction and quantitative RT-PCR

Total RNA was prepared from 10-day-old seedlings by the phenol extraction procedure and reverse transcribed using PrimeScript reverse transcriptase (Takara, Kyoto, Japan). Quantitative real-time PCR (qRT-PCR) was performed on three biological replicates using the Thermal Cycler Dice Real Time System TP-760 (Takara) with the Kapa SYBR fast universal qPCR kit (Kapa Biosystems, Boston, MA, USA). *SPMS* was used as an internal control. Each sample was duplicated in PCR reactions. Gene-specific primers used for expression analysis are listed in Table S1. Exon-intron structure of *SACL3* and the location of primers used for qRT-PCR analysis of the two splice variants are shown in Fig. S1.

Analysis of mRNA stability

For treatment with cordycepin, 7-day-old seedlings grown on agar plates were preincubated in MS liquid media with 1% sucrose for 24 h. Cordycepin (Fuji film Wako, Tokyo, Japan) was then added to the media at final concentration of 0.5 mM before RNA extraction.

GUS construction and assay

The transgenic line carrying the bacterial β-glucuronidase (*GUS*) gene fused to the *SACL3* promoter and its 5' leader is described previously [9]. For making transgenic lines expressing the *SACL3* 5' leader-*GUS* fusion gene under the control of the Cauliflower mosaic virus (CaMV) 35S promoter, a 1.4-kb genomic fragment of the *SACL3* 5' leader sequence was amplified from Arabidopsis wild-type genomic DNA by PCR using gene-specific primers (Table S1) and inserted as a *Spe*I-*Bgl*II restriction fragment into *Xba*I-*Bam*HI sites between the CaMV 35S promoter and the *GUS* gene of the pBI121 plasmid (Clontech, Palo Alto, CA, USA). The resulting T-DNA construct was introduced into the wild-type Arabidopsis genome by the floral dip method [27]. Transgenic lines were further crossed with *jmj22-2* to produce those in the *jmj22-2* mutant background.

Fluorometric assay of the GUS activity was performed as described previously [28]. The fluorescence was measured with an RF-5300PC spectrofluorophotometer (Shimadzu, Kyoto, Japan). Total protein content was measured by using the Bradford assay (BioRad, Hercules, CA, USA).

Microscopy

To examine vein development in hypocotyls and cotyledons, seedlings were fixed in a 9:1 mixture of ethanol and acetic acid, cleared with chloral hydrate as described [29], and observed under a light microscope equipped with Nomarski DIC optics (DM5000B, Leica, Wetzlar, Germany). For lignin staining, stems of 30-day-old plants were embedded in 6% agarose and sectioned with a vibratome into 50 μm-thick slices. The sections were stained with 1% (w/v) phloroglucinol in 6 M HCl for 2 min and immediately observed under a light microscope.

GO analysis

Gene ontology (GO) term enrichment analysis was performed using PANTHER biological process categories at The Arabidopsis Information Resource (TAIR, www.arabidopsis.org).

Results

sac59 is a recessive allele of *JMJ22*

Adult plants of *acl5 sac59* show a partial suppression of the *acl5* phenotype in terms of plant height while the F1 plants from the cross between *acl5 sac59* and *acl5* show the phenotype identical to *acl5* (Figs. 1A, B), indicating that *sac59* represents a recessive mutant. Lignin staining of stem sections by phloroglucinol–HCl revealed that the lignified area was reduced in *acl5 sac59* compared with that in *acl5* (Fig. 1C). The thick vein phenotype observed in *acl5* hypocotyls and cotyledons was also shown to be partially restored by *sac59* (Figs. 1D, E).

Transcript level of the mutated *ACL5* and that of many of the genes involved in xylem development are upregulated in *acl5* seedlings [30]. These include *ARABIDOPSIS THALIANA HOMEOBOX8* (*ATHB8*), which is implicated in regulating *ACL5* expression [31], *T5L1*, and *PHLOEM INTERCALATED WITH XYLEM/TDIF RECEPTOR* (*PXY/TDR*). Quantitative RT-PCR analysis revealed that these transcript levels are significantly reduced in *acl5 sac59* while the transcript level of phloem-specific *SIEVE ELEMENT OCCLUSION-RELATED1* (*SEOR1*) is unaltered in *acl5* and *acl5 sac59* (Fig. 2). We also confirmed that transcript levels of *SAC51*, *SACL1*, and *SACL2* are unaffected in in *acl5* and *acl5 sac59* while the levels of two isoforms of *SACL3*, whose exon-intron structure is shown in Fig. S1, are increased in *acl5* but restored in *acl5 sac59* (Fig. 2).

To clone the gene responsible for *sac59*, we employed fine mapping in combination with whole-genome sequencing and found that *sac59* has a point mutation in *JMJ22* (Fig. 3A). This base substitution results in an amino-acid change from Gly that is also conserved in a putative human ortholog, JMJD6, to Arg at 320 (Fig. 3B). A T-DNA insertion allele of *JMJ22* has previously been designated as *jmj22-1* [32]. We obtained another T-DNA insertion allele from ABRC, named *jmj22-2* (Fig. 3A), and examined whether *jmj22-2* suppresses the *acl5* phenotype or not. The result showed that the dwarf phenotype of *acl5-1* is suppressed by homozygous *jmj22-2* but not by heterozygous *jmj22-2* (Fig. 3C). Since the *acl5* plants heterozygous for *jmj22-2* and *sac59* also clearly restored the plant height, we concluded that *sac59* is an allele of *JMJ22* and hereafter renamed *jmj22-3*. We confirmed that the *jmj22-3* single mutant shows no morphological abnormalities under our experimental conditions and

transcript levels of *ACL5*, *ATHB8*, *T5L1*, *PXY/TDR*, *SEOR1*, and all members of the *SAC51* family in *jmj22-3* seedlings are comparable to those in wild-type seedlings (Fig. 2).

jmj20 jmj21 jmj22 triple mutants show normal morphology

The Arabidopsis JmjC protein genes can be categorized into five classes and the class that putatively corresponds to the mammalian JMJD6 class contains *JMJ21* and *JMJ22* [20]. Our phylogenetic analysis revealed that a putative ortholog of *JMJ22* is also present in the spikemoss *Selaginella* and the liverwort *Marchantia* but that of *JMJ21* is not in *Marchantia* (Fig. 4A). To examine the functional relationship between *JMJ22* and *JMJ21*, we generated a knockout mutant of *JMJ21* by genome editing technology. One mutant that has a 1.5-kb deletion in *JMJ21* was obtained and named *jmj21-1* (Fig. 4B). *jmj21-1* shows normal growth and *acl5 jmj21-1* plants are identical to *acl5* in appearance (Fig. 4C). We further crossed these mutants with *jmj20-2*, a T-DNA insertion mutant of *JMJ20* (Fig. 4B), which is the second closest homolog of *JMJ22* but belongs to the JmjC domain-only class [20]. The results revealed that *jmj20-2 jmj21-1 jmj22-2* shows normal growth and morphology, and *jmj20-2* has no suppressive effect on the *acl5* phenotype (Fig. 4C). We confirmed that these T-DNA insertion and genome-edited mutants have no transcript encompassing their respective mutation sites but have reduced levels of the transcripts upstream of and probably truncated by the mutations (Fig. S2).

While many of the JmjC domain-containing proteins have been characterized as histone demethylases, those of the JMJD6 class have been reported to interact with multiple protein substrates in distinct molecular pathways or directly with RNA, and their function remains controversial in mammals [12]. The search of ATTED-II, a database of co-expressed genes in Arabidopsis [33], indicates that, unlike *JMJ21* and *JMJ20*, *JMJ22* may be associated with the genes for RNA binding proteins and ribosomal proteins (Table S2). GO analysis confirms that the genes related to rRNA processing are highly enriched in the top 50 or 100 genes co-expressed with *JMJ22* while they are not with *JMJ21* and *JMJ20* (Tables 1 and S3).

The *acl5 sacl3* phenotype is not suppressed by *jmj22*

To examine whether suppression of the *acl5* phenotype by the *jmj22* mutation involves the function of *SAC51* family proteins, we generated triple mutants of *acl5 jmj22-2 sac51-1* and *acl5 jmj22-2 sacl3-1*. As shown previously [9], *acl5 sac51-1* is morphologically identical to *acl5* while *acl5 sacl3-1* has a very tiny size of inflorescences and leaves (Fig. 5). We found

that the *acl5* phenotype of *acl5 sac51-1* is partially suppressed by *jmj22-2* as observed in the case of the *acl5* single mutant but the tiny plant phenotype of *acl5 sacl3-1* is not suppressed by *jmj22-2* (Fig. 5).

The mRNAs of the *SAC51* family are stabilized by *jmj22*

The above results raise the possibility that the *acl5* phenotype is suppressed through the enhancement of translation of the *SACL3* mRNA in the *jmj22* mutant. We thus examined whether it is affected by *jmj22* or not, by using the GUS reporter gene fused to the *SACL3* 5' leader, which contains a conserved uORF. Fusion genes expressed under the *SACL3* own promoter and the CaMV 35S promoter were introduced into the wild type and then transferred to *jmj22-2* by the crosses, respectively. The results, however, revealed no significant difference of the GUS activity between wild-type and *jmj22-2* seedlings as for both fusion constructs (Fig. 6A).

We have previously shown that translation of the *SAC51* 5' leader-GUS fusion transcript is enhanced by *acl5* suppressors, *sac52-d*, *sac53-d*, and *sac56-d* and the *SAC51* mRNA is stabilized by these mutations and thermospermine [6, 7]. We examined the effect of the *jmj22* mutation on the mRNA stability of the *SAC51* family genes. Ten-day-old seedlings were treated with 0.5 mM cordycepin to inhibit RNA synthesis and subjected to qRT-PCR analysis. The results revealed that the *SAC51* mRNA is degraded more slowly in *acl5 jmj22-2* than in *acl5* seedlings (Fig. 6B). Significant enhancement of the mRNA stability was detected in all members of the *SAC51* family including two alternative spliced variants of the *SACL3* mRNA (Fig. 6B).

Discussion

Given the fact that a T-DNA insertion mutant, *jmj22-2*, and an amino acid substitution mutant, *jmj22-3*, which we originally identified as *sac59*, have the same suppressive effect on the *acl5* phenotype, both may represent loss-of-function alleles. We have further generated a knockout allele of *JMJ21*, the closest homolog of *JMJ22*, but the double knockout of *jmj21 jmj22* and the triple knockout with *jmj20* were found to exhibit normal growth and morphology. It is thus concluded that these genes are not essential for viability, although the possibility should not be excluded of the presence of additional genes that can function redundantly with these *JMJ* genes. It is also possible that these genes are required under certain environmental conditions. In *Drosophila*, most *JmjC* genes do not critically regulate development as the mutants of 10

out of all 13 members show no obvious developmental defects, and they are suggested to generally fine-tune different biological processes [34].

According to a previous study, the seeds of *jmj20-1 jmj22-1* show a reduced germination efficiency after a red light-pulse treatment while these plants display wild-type phenotypes throughout vegetative development under standard growth conditions [32]. The study suggested that JMJ20 and JMJ22 act redundantly as positive regulators of seed germination through the removal of repressive histone arginine methylations at gibberellic acid-biosynthetic genes. Although we have not addressed the effect of these mutations on histone modification, our results with the co-expression data rather suggest that JMJ22 has a different function from JMJ20. Phylogenetic analysis at least indicates that JMJ20 is not a member of the JMJD6 class but belongs to the JmjC domain-only class [20, 21]. This class also contains JMJ30, JMJ31, and JMJ32. JMJ30 and JMJ32 have been shown to function as H3K27 demethylases at elevated temperatures and derepress expression of the flowering repressor, *FLC*, and a subset of heat-shock protein genes [35, 36]. On the other hand, JMJ21 and JMJ22 belong to the JMJD6 class. However, it is also likely that these two proteins have functionally diverged from each other. It is noted that the JmjC domain of JMJ21 is followed by a long peptide sequence that is not present in JMJ22 and mammalian JMJD6 [20]. A deletion mutant of *JMJ21* generated in this study will provide a useful tool for further analysis of this gene, which may be unique to vascular plants (Fig. 3A).

The results of gene expression analyses revealed that the levels of xylem- and cambium-specific genes up-regulated in *acl5* were reduced by *jmj22*, correlating with the degree of restoration of xylem development, while those of *SAC51* family genes except *SACL3* showed no correlation with the vascular phenotype (Fig. 2). Together with the result that these transcripts were stabilized by *jmj22* in *acl5*, that is, in the absence of thermospermine (Fig. 6), the longevity of these transcripts may be crucial to suppress the *acl5* phenotype. Importantly, we confirmed that the *jmj22* mutation cannot suppress the tiny-plant phenotype of *acl5 sacl3* at all while it suppresses the phenotype of *acl5 sac51*, suggesting that the importance of *SACL3* in the suppression of the *acl5* phenotype by *jmj22*. According to a previous study [37], both *SACL3* and *SAC51* mRNAs have been identified as a target of nonsense-mediated mRNA decay (NMD) because these mRNA levels are elevated in NMD mutants. NMD can be avoided if a ribosome wipes out the exon-junction complexes during the first round of translation. In *sac52-d*, *sac53-d*, and *sac56-d* mutants whose responsible genes code for ribosomal proteins RPL10, RACK1, and RPL5, respectively, the *SAC51* mRNA level is more stabilized probably because these ribosomal mutations enhance translation of the *SAC51* main ORF instead of thermospermine, thereby making the *SAC51* mRNA escaped from NMD [7]. Considering a

close link of JMJ22 with mRNA processing shown by the GO analysis of the co-expressed genes, JMJ22 might be involved in the NMD-mediated quality control of *SAC51* family mRNAs. However, it remains unclear whether the *jmj22* mutation has an enhancing effect on translation of these *SAC51* family mRNAs or not. The GUS reporter activity derived from the *SACL3* 5' leader-GUS transgene was not increased by *jmj22-2*. The translational activity of the *SACL3* mRNA might not have been reproduced in the *SACL3-GUS* chimeric mRNA used in this study. Some studies in mammals have reported on the involvement of JMJD6 in mRNA splicing [12, 38]. Reduced *JMJD6* expression increases accumulation of an alternative splice variant of some mRNAs leading either to those subjected to NMD or expression of truncated proteins. In this study, we have detected no difference of the effect of *jmj22* on the fate of two alternative isoforms of the *SACL3* mRNA. It is still possible, however, that additional alternative spliced mRNAs of *SACL3* are produced in the *jmj22* mutant.

In summary, our results revealed that a plant JMJD6, JMJ22, has a role in proper xylem formation probably through modulating the fate of *SAC51* family mRNAs. Although its precise function remains unsolved, it is unlikely that JMJ22 is specifically involved in the process of xylem development, considering the functions of JMJD6 reported for animals and yeast [12-16]. Global transcriptomic analysis of *jmj22* as well as *jmj21* mutants could help to elucidate the mode of action of plant JMJD6.

Declarations of Competing Interest

None.

Acknowledgements

This work was supported in part by the Japan Society for the Promotion of Science (JSPS) Grants-in-Aid for Scientific Research (Nos. 19K06724) to T.T.

Data Availability

The data that support the findings of this study and all plant materials are available from the corresponding author [perfect@cc.okayama-u.ac.jp] upon reasonable request.

References

1 Oshima T. A new polyamine, thermospermine, 1,12-diamino-4,8-diazadodecane, from an extreme thermophile. *J Biol Chem.* 1979;**254:**8720-2.

2 Takano A, Kakehi J-I, Takahashi T. Thermospermine is not a minor polyamine in the plant kingdom. *Plant Cell Physiol.* 2012;**53:**606-16.

3 Kakehi J-I, Kuwashiro Y, Niitsu Y, Takahashi T. Thermospermine is required for stem elongation in *Arabidopsis thaliana*. *Plant Cell Physiol.* 2008;**49:**1342-9.

4 Clay NK, Nelson T. *Arabidopsis thickvein* mutation affects vein thickness and organ vascularization, and resides in a provascular cell-specific spermine synthase involved in vein definition and in polar auxin transport. *Plant Physiol.* 2005;**138:**767-77.

5 Imai A, Hanzawa Y, Komura M, Yamamoto KT, Komeda Y, Takahashi T. The dwarf phenotype of the *Arabidopsis acl5* mutant is suppressed by a mutation in an upstream ORF of a bHLH gene. *Development.* 2006;**133:**3575-85.

6 Imai A, Komura M, Kawano E, Kuwashiro Y, Takahashi T. A semi-dominant mutation in the ribosomal protein L10 gene suppresses the dwarf phenotype of the *acl5* mutant in *Arabidopsis*. *Plant J.* 2008;**56:**881-90.

7 Kakehi J-I, Kawano E, Yoshimoto K, Cai Q, Imai A, Takahashi T. Mutations in ribosomal proteins, RPL4 and RACK1, suppress the phenotype of a thermospermine-deficient mutant of *Arabidopsis thaliana*. *PLoS One.* 2015;**27:**e0117309.

8 Vera-Sirera F, De Rybel B, Úrbez C, Kouklas E, Pesquera M, Álvarez-Mahecha JC, et al. A bHLH-based feedback loop restricts vascular cell proliferation in plants. *Dev Cell.* 2015;**35:**432-43.

9 Cai Q, Fukushima H, Yamamoto M, Ishii N, Sakamoto T, Kurata T, et al. The SAC51 family plays a central role in thermospermine responses in Arabidopsis. *Plant Cell Physiol.* 2016;**57:**1583-92.

10 Ohashi-Ito K, Fukuda H. Functional mechanism of bHLH complexes during early vascular development. *Curr Opin Plant Biol.* 2016;**33:**42-7.

11 Katayama H, Iwamoto K, Kariya Y, Asakawa T, Kan T, Fukuda H, et al. A negative feedback loop controlling bHLH complexes is involved in vascular cell division and differentiation in the root apical meristem. *Curr Biol.* 2015;**25:**3144-50.

12 Kwok J, O'Shea M, Hume DA, Lengeling A. Jmjd6, a JmjC Dioxygenase with many interaction partners and pleiotropic functions. *Front Genet.* 2017;**8:**32.

13 Lawrence P, Rieder E. Insights into Jumonji C-domain containing protein 6 (JMJD6): a multifactorial role in foot-and-mouth disease virus replication in cells. *Virus Genes.* 2017;**53:**340-51.

14 Vangimalla SS, Ganesan M, Kharbanda KK, Osna NA. Bifunctional enzyme JMJD6 contributes to multiple disease pathogenesis: new twist on the old story. *Biomolecules*. 2017;**7:**41.

15 Yang J, Chen S, Yang Y, Ma X, Shao B, Yang S, et al. Jumonji domain-containing protein 6 protein and its role in cancer. *Cell Prolif.* 2020;**53:**e12747.

16 Wong M, Sun Y, Xi Z, Milazzo G, Poulos RC, Bartenhagen C, et al. JMJD6 is a tumorigenic factor and therapeutic target in neuroblastoma. *Nat Commun.* 2019;**10:**3319.

17 Hahn P, Wegener I, Burrells A, Böse J, Wolf A, Erck C, et al. Analysis of Jmjd6 cellular localization and testing for its involvement in histone demethylation. *PLoS One.* 2010;**5:**e13769.

18 Hong X, Zang J, White J, Wang C, Pan CH, Zhao R, et al. Interaction of JMJD6 with single-stranded RNA. *Proc Natl Acad Sci USA.* 2010;**107:**14568-72.

19 Liu W, Ma Q, Wong K, Li W, Ohgi K, Zhang J, et al. Brd4 and JMJD6-associated anti-pause enhancers in regulation of transcriptional pause release. *Cell.* 2013;**155:**1581-95.

20 Lu F, Li G, Cui X, Liu C, Wang XJ, Cao X. Comparative analysis of JmjC domain-containing proteins reveals the potential histone demethylases in *Arabidopsis* and rice. *J Integr Plant Biol.* 2008;**50:**886-96.

21 Huang Y, Chen D, Liu C, Shen W, Ruan Y. Evolution and conservation of JmjC domain proteins in the green lineage. *Mol Genet Genomics.* 2016;**291:**33-49.

22 Hanzawa Y, Takahashi T, Michael AJ, Burtin D, Long D, Pineiro M, et al. *ACAULIS5*, an *Arabidopsis* gene required for stem elongation, encodes a spermine synthase. *EMBO J.* 2000;**19:**4248-56.

23 Konieczny A, Ausubel FM. A procedure for mapping *Arabidopsis* mutations using co-dominant ecotype-specific PCR-based markers. *Plant J.* 1993;**4:**403-10.

24 Bell CJ, Ecker JR. Assignment of 30 microsatellite loci to the linkage map of *Arabidopsis*. *Genomics*. 1994;**19:**137-44.

25 Tanaka T, Nishii Y, Matsuo H, Takahashi T. Easy-to-use InDel markers for genetic mapping between Col-0 and L*er*-0 accessions of *Arabidopsis thaliana*. *Plants*. 2020;**9:**779.

26 Fauser F, Schiml S, Puchta H. Both CRISPR/Cas-based nucleases and nickases can be used efficiently for genome engineering in *Arabidopsis thaliana*. *Plant J.* 2014;**79:**348-59.

27 Clough SJ, Bent AF. Floral dip: a simplified method for Agrobacterium-mediated transformation of *Arabidopsis thaliana*. *Plant J.* 1998;**16:**735-43.

28 Jefferson RA, Kavanagh TA, Bevan MW. GUS fusions: β-glucuronidase as a sensitive and versatile gene fusion marker in higher plants. *EMBO J.* 1987;**6:**3901-7.

29 Yoshimoto K, Noutoshi Y, Hayashi K, Shirasu K, Takahashi T, Motose H. A chemical biology approach reveals an opposite action between thermospermine and auxin in xylem development in *Arabidopsis thaliana*. *Plant Cell Physiol.* 2012;**53:**635-45.

30 Tong W, Yoshimoto K, Kakehi J, Motose H, Niitsu M, Takahashi T. Thermospermine modulates expression of auxin-related genes in *Arabidopsis*. *Front Plant Sci.* 2014;**5:**94.

31 Baima S, Forte V, Possenti M, Peñalosa A, Leoni G, Salvi S, et al. Negative feedback regulation of auxin signaling by ATHB8/ACL5-BUD2 transcription module. *Mol. Plant.* 2014;**7:**1006-1025.

32 Cho JN, Ryu JY, Jeong YM, Park J, Song JJ, Amasino RM, et al. Control of seed germination by light-induced histone arginine demethylation activity. *Dev Cell.* 2012;**22:**736-48.

33 Obayashi T, Kinoshita K, Nakai K, Shibaoka M, Hayashi S, Saeki M, et al. ATTED-II: a database of co-expressed genes and cis elements for identifying co-regulated gene groups in *Arabidopsis*. *Nucleic Acids Res.* 2007;**35:**D863-9.

34 Shalaby NA, Sayed R, Zhang Q, Scoggin S, Eliazer S, Rothenfluh A, et al. Systematic discovery of genetic modulation by Jumonji histone demethylases in *Drosophila*. *Sci Rep.* 2017;**7:**5240.

35 Gan ES, Xu Y, Wong JY, Goh JG, Sun B, Wee WY, et al. Jumonji demethylases moderate precocious flowering at elevated temperature via regulation of *FLC* in *Arabidopsis*. *Nat Commun.* 2014;**5:**5098.

36 Yamaguchi N, Matsubara S, Yoshimizu K, Seki M, Hamada K, Kamitani M, et al. H3K27me3 demethylases alter *HSP22* and *HSP17.6C* expression in response to recurring heat in *Arabidopsis*. *Nat Commun.* 2021;**12:**3480.

37 Rayson S, Arciga-Reyes L, Wootton L, De Torres Zabala M, Truman W, Graham N, et al. A role for nonsense-mediated mRNA decay in plants: pathogen responses are induced in *Arabidopsis thaliana* NMD mutants. *PLoS One.* 2012;**7:**e31917.

38 Webby CJ, Wolf A, Gromak N, Dreger M, Kramer H, Kessler B, et al. Jmjd6 catalyses lysyl-hydroxylation of U2AF65, a protein associated with RNA splicing. *Science.* 2009;**325:**90-3.

39 Chevenet F, Brun C, Bañuls AL, Jacq B, Christen R. TreeDyn: towards dynamic graphics and annotations for analyses of trees. *BMC Bioinformatics.* 2006;**7:**439.

Figure legends

Fig. 1. Phenotype of the *sac59* mutant. (A) and (B) Gross morphological comparison of 30-day-old (A) and 42-day-old (B) plants of wild-type (Wt) and each mutant with L*er* background. *sac59/+* indicates heterozygotes of *sac59* and wild-type alleles. Bars = 5 cm. (C) Stem sections of 30-day-old plants that were stained with phloroglucinol-HCl. (D) and (E) Hypocotyls (D) and cotyledons (E) of 7-day-old seedlings cleared with chloral hydrate. Bars in (C), (D), and (E) = 200 μm.

Fig. 2. Effect of *sac59* on gene expression. Relative mRNA levels of *ACL5, T5L1, ATHB8, TDR, SEOR1,* and all members of the *SAC51* family in 10-day-old seedlings grown in MS plates were examined by quantitative RT-PCR. *SACL3I* and *SACL3II* represent two alternatively spliced forms of *SACL3* (Fig. S1). mRNA levels were normalized to the *SPMS* mRNA level and set to 1 in wild type (Wt). Values are means ± SE (n = 6). Different letters indicate significant differences at $P < 0.05$ by ANOVA.

Fig. 3. *sac59* is allelic to *jmj22-2*. (A) Exon-intron structure of *JMJ22*. Black boxes represent coding regions. T-DNA insertion sites in *jmj22-1* and *jmj22-2* and the site of a point mutation in *sac59* (hereafter *jmj22-3*) are indicated by triangles and an asterisk, respectively. (B) Alignment of amino acid sequence around the mutation site of *jmj22-3* with the corresponding sequences of JMJD6 proteins of different organisms. Numbers indicate the first amino acid residues of the shown sequences. Asterisks indicate amino acids identical to AtJMJ22. At, *Arabidopsis thaliana*; Sm, *Selaginella moellendorffii*; Cr, *Chlamydomonas reinhardtii*; Hs, *Homo sapiens*. (C) Gross morphological comparison of 42-day-old plants of wild-type (Wt) and each mutant with Col-0 background. Plus indicates wild-type allele.

Fig. 4. The *acl5* phenotype is not suppressed by *jmj20* and *jmj21* mutations. (A) Phylogenetic relationship among Arabidopsis JMJ20, JMJ21, JMJ22, and the related JMJ proteins of other organisms. At, *Arabidopsis thaliana*; Sm, *Selaginella moellendorffii*; Os, *Oryza sativa*; Mp, *Marchantia polymorpha*; Hs, *Homo sapiens*. The tree was generated by using CLUSTAL W and TreeDyn [39]. The scale bar represents the evolutionary distance in the units of the number of amino acid substitutions per site. (B) Exon-intron structure of *JMJ21* and *JMJ20*. Black boxes represent coding regions. The region deleted by genome editing in *jmj21-1* and T-DNA insertion sites in *jmj20-1* and *jmj20-2* are indicated by a dashed line and triangles, respectively. (C) Plant height comparison of 40-day-old plants of wild-type (Wt) and each mutant with Col-

0 background. Values are means ± SE (n = 6). Different letters indicate significant differences at $P < 0.05$ by ANOVA.

Fig. 5. Effect of *jmj22-2* on the phenotype of *acl5 sacl3-1*. (A) Gross morphology of 30-day-old plants of each mutant. Bars = 1 cm. (B) Comparison of the first foliage leaf of 25-day-old plants of each mutant. Bar = 1 cm.

Fig. 6. Effect of *jmj22-2* on the *SACL3* 5'-GUS expression and the mRNA stability of *SAC51* family genes. (A) Relative GUS activity in 7-day-old seedlings of wild-type (Wt) and *jmj22-2* backgrounds carrying the *SACL3* 5'-*GUS* fusion gene expressed under the *SACL3* promoter (*L3* pro+*L3* 5'+*GUS*) or CaMV 35S promoter (*35S*+*L3* 5'+*GUS*). Values are means ± SE (n = 3). (B) Relative mRNA levels of *SAC51* family genes after treatment of 8-day-old seedlings of *acl5* and *acl5 jmj22-2* with 0.5 mM cordycepin. Values are means ± SE (n = 3). Asterisks indicate significant difference from *acl5* at the same time point of the treatment. ($P < 0.05$, *t* test).

Table 1

Gene ontology analysis of the top 50 co-expressed genes of *JMJ22*.

GO term	Gene #/50	B.G. (% of 27,416)	Fold enrichment	P-value
GO:0006364 rRNA processing	20	254 (0.93)	43.17	4.86E-24
GO:0016072 rRNA metabolic process	20	263 (0.96)	41.7	9.41E-24
GO:0042254 ribosome biogenesis	21	370 (1.35)	31.12	1.28E-22
GO:0034470 ncRNA processing	20	381 (1.39)	28.78	1.09E-20
GO:0022613 ribonucleoprotein complex biogenesis	21	447 (1.63)	25.76	5.65E-21
GO:0034660 ncRNA metabolic process	20	455 (1.66)	24.1	3.21E-19
GO:0006396 RNA processing	22	787 (2.87)	15.33	1.84E-17
GO:0016070 RNA metabolic process	23	1294 (4.71)	9.75	3.35E-14
GO:0044085 cellular component biogenesis	22	1325 (4.83)	9.1	8.92E-13
GO:0010467 gene expression	23	1608 (5.87)	7.84	3.49E-12
GO:0090304 nucleic acid metabolic process	23	1705 (6.21)	7.4	1.21E-11
GO:0006139 nucleobase-containing compound metabolic process	24	2093 (7.63)	6.29	8.25E-11
GO:0046483 heterocycle metabolic process	24	2393 (8.72)	5.5	1.50E-09
GO:0006725 cellular aromatic compound metabolic process	24	2519 (9.19)	5.22	4.51E-09
GO:0071840 cellular component organization or biogenesis	26	2813 (10.26)	5.07	6.13E-10
GO:1901360 organic cyclic compound metabolic process	24	2607 (9.51)	5.05	9.39E-09
GO:0034641 cellular nitrogen compound metabolic process	25	2872 (10.48)	4.77	8.83E-09

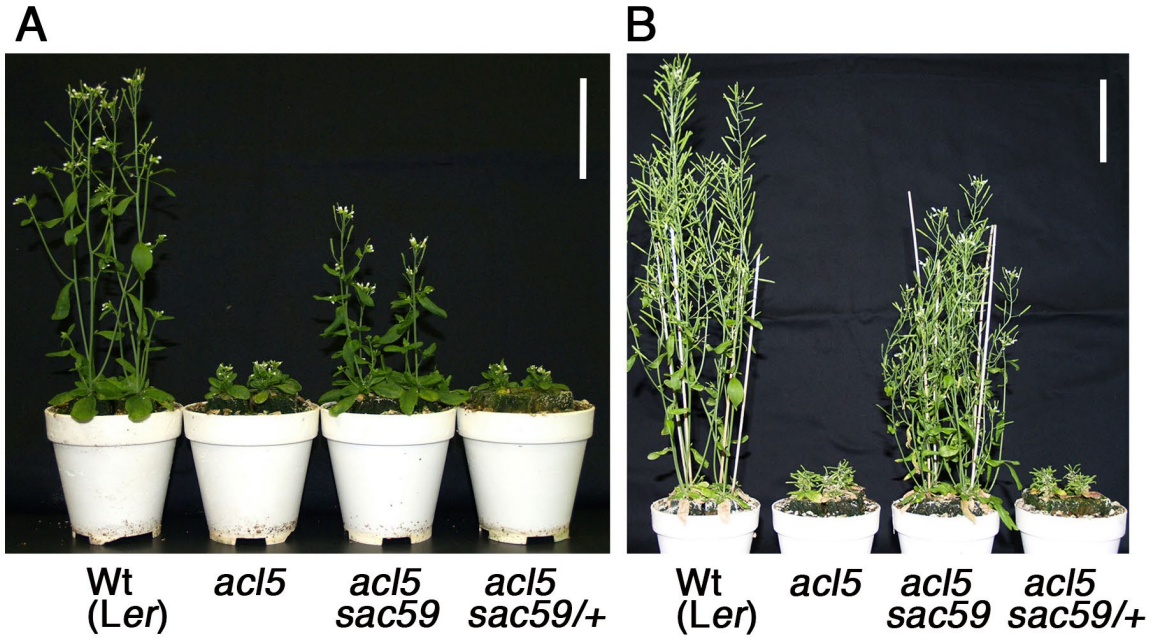
A
B
Wt (Ler)
acl5
acl5 sac59
acl5 sac59/+
Wt (Ler)
acl5
acl5 sac59
acl5 sac59/+

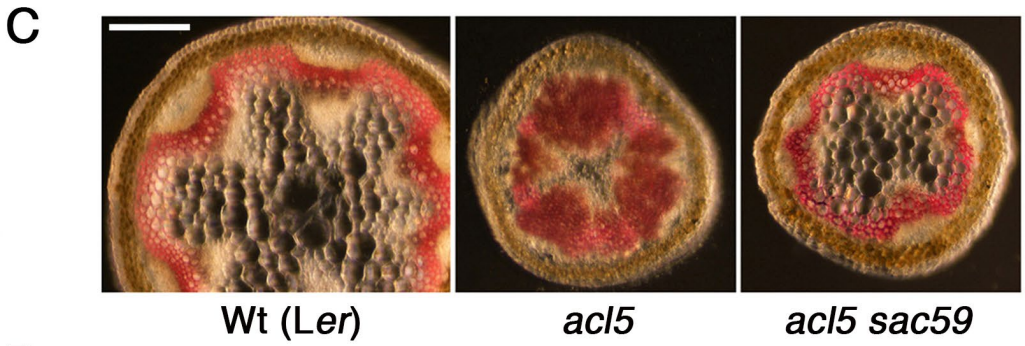
C
Wt (Ler)
acl5
acl5 sac59

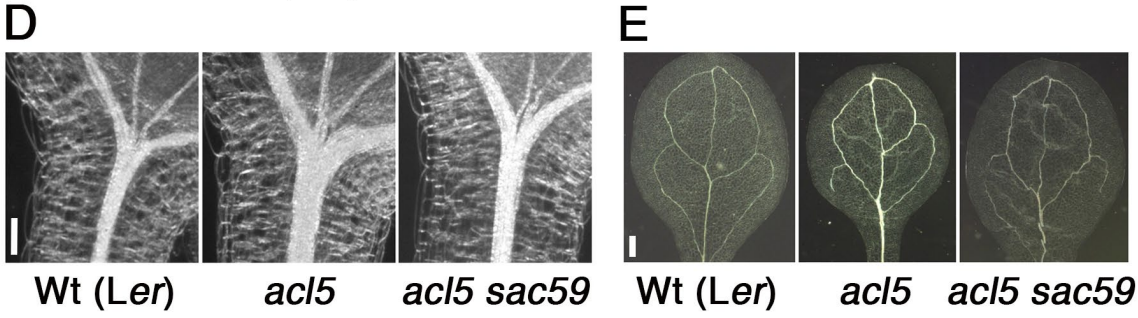
D
E
Wt (Ler)
acl5
acl5 sac59
Wt (Ler)
acl5
acl5 sac59

Figure 1

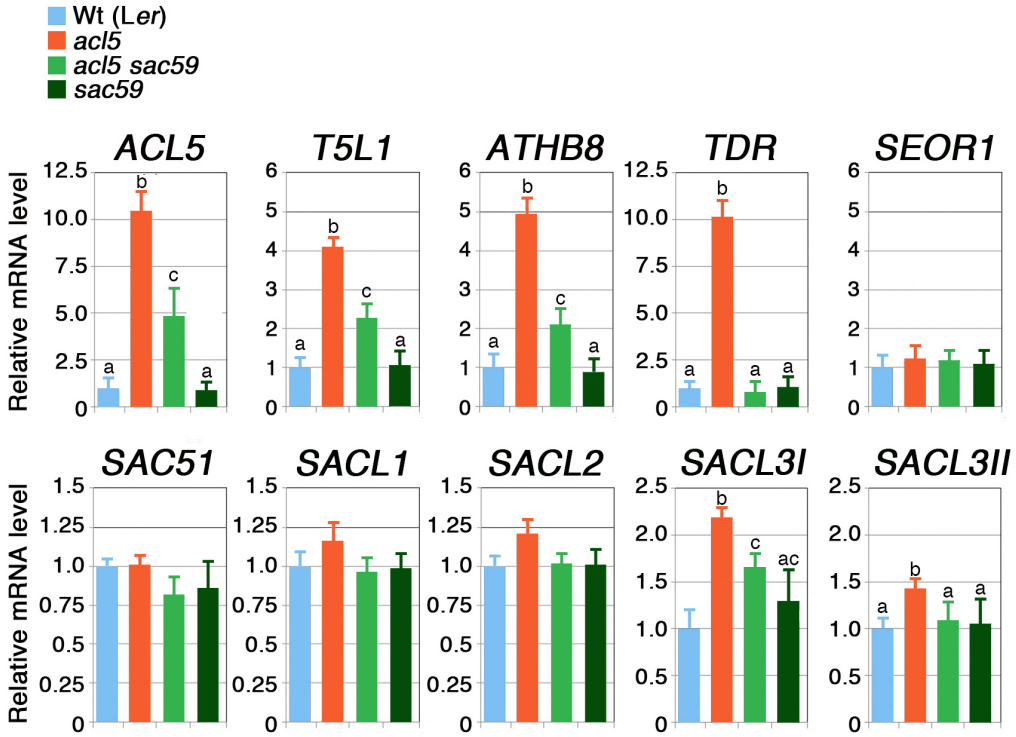

Figure 2

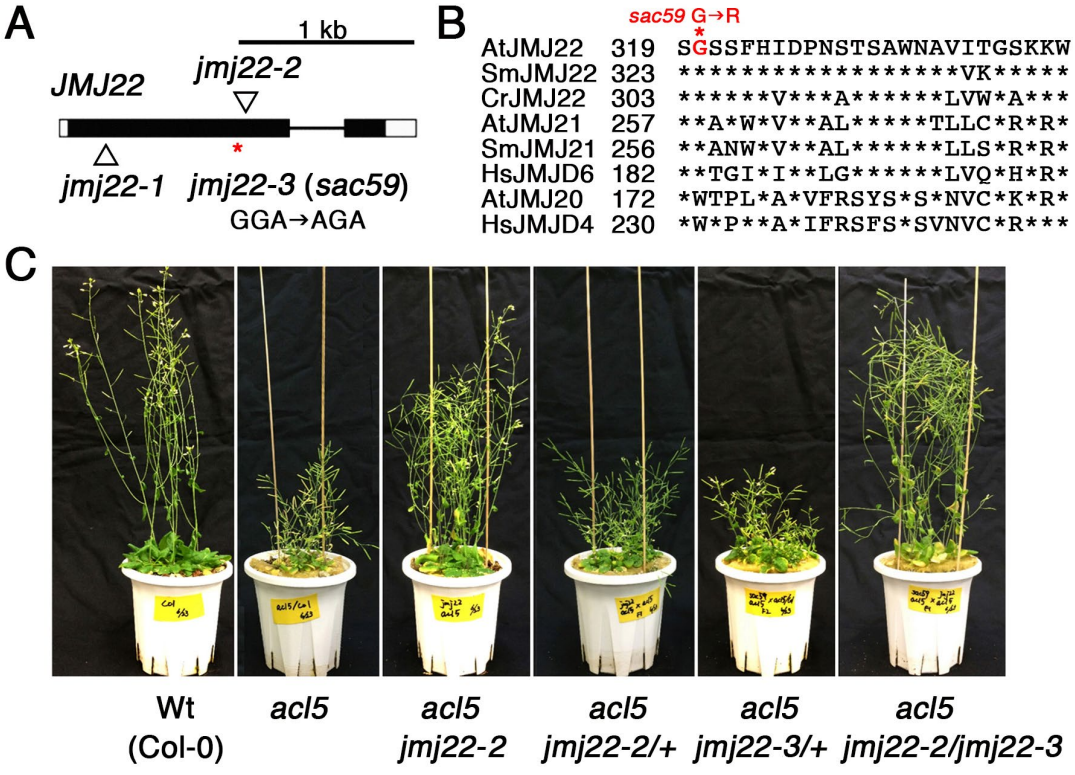

Figure 3

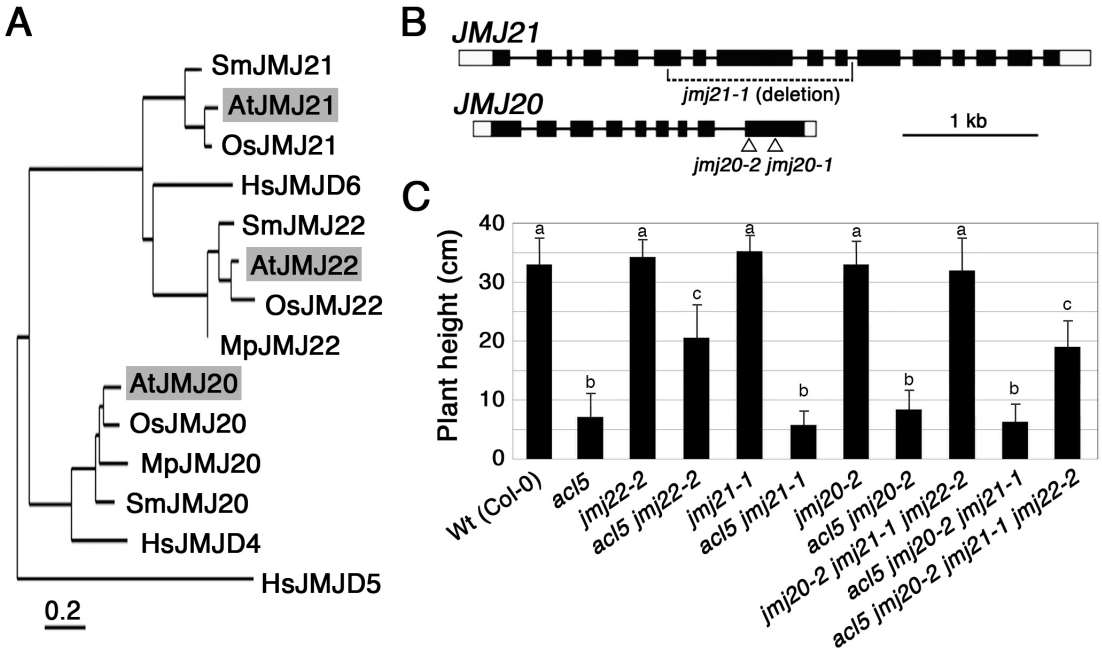

Figure 4

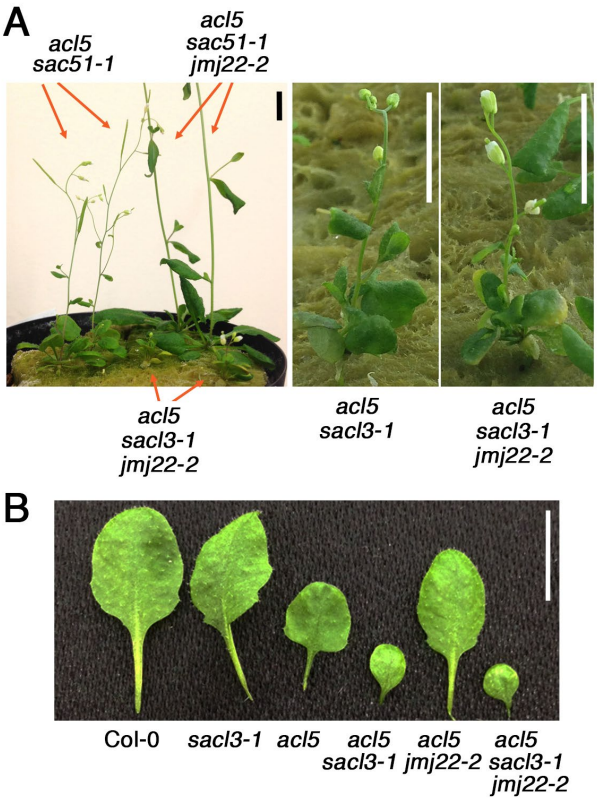

Figure 5

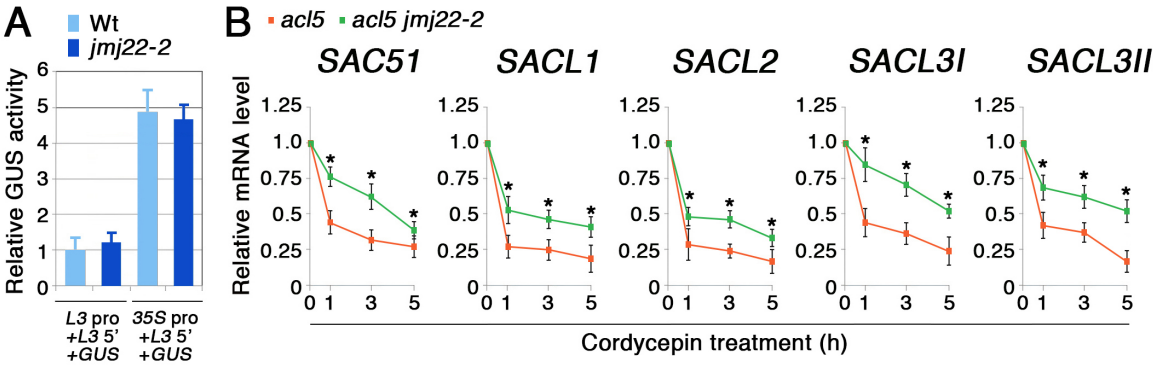
A
Wt
jmj22-2
Relative GUS activity
0
1
2
3
4
5
6
L3 pro +L3 5' +GUS
35S pro +L3 5' +GUS
B
acl5
acl5 jmj22-2
SAC51
SACL1
SACL2
SACL3I
SACL3II
Relative mRNA level
0
0.25
0.5
0.75
1.0
1.25
0 1 3 5
Cordycepin treatment (h)

Figure 6